Contents lists available at ScienceDirect

Surface & Coatings Technology

Development of new decorative coatings based on gold nanoparticles dispersed in an amorphous TiO$_2$ dielectric matrix

M. Torrell [a,*], P. Machado [a], L. Cunha [a], N.M. Figueiredo [b], J.C. Oliveira [b], C. Louro [b], F. Vaz [a]

[a] Universidade do Minho, Dept. Física, Campus de Azurém, 4800-058 Guimarães, Portugal
[b] SEC-CEMUC-Universidade de Coimbra, Dept. Eng. Mecânica, Polo II, 3030-788 Coimbra, Portugal

ARTICLE INFO

ABSTRACT

The present work is devoted to the optical properties of Au:TiO$_2$ thin films in order to clarify the role of the Au clusters inclusions in the TiO$_2$ dielectric matrix. Three series of films containing about 30 at.% (29.2), 20 at.% (19.8) and 10 at.% (9.3) Au were deposited by dc reactive magnetron sputtering.

On thermal annealing in the range from 300 to 800 °C in protective atmosphere, significant changes on the crystalline phases and clusters dimensions were detected. The most promising optical behavior was found for the film 20% Au:TiO$_2$, where the films revealed some colour changes, evolving from several shades of grey to different tones of red. This change in the optical behaviour of the films was found to be correlated with a cluster size increase from 2 to 17 nm. For higher size values (>20 nm) the films, independently of the Au content, showed a golden appearance colour. The optical changes were confirmed by reflectivity and CIELab colour measurements. Regarding the films with 10 and 30 at.% Au, the results confirmed that there is an evident range of compositions and clusters size where the SPR is more evident. Sample A (10 at.% Au) it seems to be in the lower limit of the SPR showing a typical interferometric behavior on the reflectivity measurements, similar to the TiO$_2$ optical behavior. Regarding the 30 at.% Au one, the results seems to indicate that the amount of gold particles and their grain size is in the upper limit to show a SPR activity.

© 2009 Elsevier B.V. All rights reserved.

1. Introduction

The interband transitions (d band to the s–p conduction band) at shorter wavelengths and the intraband absorption (free electron) at longer wavelengths, are known to rule the optical properties of bulk noble metals. One interesting feature is set when a noble metal is placed in a certain type of media, as it is the case of dielectric matrixes like that of titanium oxide, TiO$_2$. In fact, metallic nanoparticles, sometimes referred to as metal clusters or nanoparticles, are being increasingly studied to be applied in many fields of modern technology, which may range from simple decorative purposes (let us recall that few centuries ago, gold particles provided color for roman glasses and medieval cathedrals windows), towards more technological ones, such as those of optics, biomedicine, optoelectronics, biosensors, magnetic storage, energy conversion, optical filters, etc. [1–4].

In scientific terms, the preparation of materials where these nanoparticles are dispersed in dielectric media (latex, polystyrene, thiol- and disulfide monolayers, sodium citrate aqueous colloid solution [5], TiO$_2$ [6], SiO$_2$ [7] etc…), are actually becoming one of the most important fields in some specific areas of materials science, and one of the new aims of the nanoscience and nanotechnology. The importance of these types of nanocomposites arises from two tunable parameters. First, the individual nanoparticle used as elementary building blocks may have size or shape-dependent properties. Second, the interparticle spacing can be modified through metal nanoparticles concentration within the host matrix, since it is affected from the geometry or the volume fraction [1–4]. Anyway, only metals with free electrons (essentially Au, Ag and Cu) lead to interesting changes on the optical properties due to the resonances in the visible spectrum, which give rise to intense colors.

In the particular case of the optical properties (the driving force in the present work), their behavior depends strongly upon the nanoparticles morphology [1]. The absorption spectrum is dominated by the resonant coupling of the incident field with quanta of collective conduction electron plasma oscillations, instead of monotonically increasing with wavelength. This resonance is called Surface Plasmon Resonance (SPR), and it is dependent on the concentration, size and shape of the metal clusters and, of course, on the dielectric properties of the surrounding medium [8,9]. The impact of these parameters is due to the changes of the frequency, when the conduction electrons oscillate in response to the alternating electric field of an incident electromagnetic radiation [10]. An interesting example of such behavior is expected to be obtained by the material resulting from the dispersion of gold clusters within a dielectric matrix of titania, TiO$_2$(Au). This composite media exhibit strong changes on the optical, electric and magnetic properties, which are not present neither in the bulk material [11], not in the correspondent metallic particles.

* Corresponding author.
E-mail address: marc.faro@fisica.uminho.pt (M. Torrell).

Taking this into account, and within the frame of the present work, gold was selected as clustering metal due to its quasi-free-electron behavior in the UV–visible spectral range; while titanium dioxide was used as dielectric matrix, owing to the inherent high refractive index and good stability [12]. With the combination of these two materials, the main objective of the present study is to use the shifts on the SP frequency to produce films with different optical properties responses. For that, magnetron sputtered Au:TiO₂ films with different Au contents were prepared and annealed at different temperatures (in vacuum) to study the influence of different structural arrangements (promoted by the thermal annealing) in their optical properties. Since the optical properties of nanoparticles dispersed into dielectric matrixes are related to their morphology and volume fraction, it is expected that the thermal treatments can modify these parameters and, consequently, the optical properties of the sputter-deposited Au:TiO₂ films.

2. Experimental details

The Au:TiO₂ thin films were deposited into silicon (100) and glass substrates by dc reactive magnetron sputtering, in a laboratory-sized deposition apparatus. Two vertically opposed rectangular magnetrons (unbalanced of type 2) were disposed in a closed field configuration in the deposition chamber. Only one electrode was powered, composed of a titanium target (99.6% purity) with varied amounts of Au pellets (20 mm² surface area and ~2 mm thickness), which were symmetrically incrusted in its preferential eroded zone (denominate hereafter as Ti—Au target). The number of Au pellets was varied in total amounts of 6, 4 and 2, giving rise to three series of films with different chemical compositions. Substrate holder was positioned at 70 mm from the Ti–Au target in all the runs, using a constant dc current density of 100 A m². A mixture of argon (flux constant of 60 sccm) and oxygen (flow set to 10 sccm) was used, being the partial pressure of oxygen in the reactive mixture of 7.9×10^{-2} Pa. The total working pressure was approximately constant during the depositions (varying only slightly between 0.4 and 0.5 Pa), with a vacuum pumping speed adjusted for 356 Ls⁻¹. The substrates were biased (-50 V) and the deposition temperature was set to a value of 200 °C. The temperature of the coated substrates was monitored with a thermocouple placed close to the surface of the substrate holder. A delay time of 5 min was employed before positioning the surface of the samples in front of the Ti–Au target. This procedure was used in order to avoid films poisoning resulting from previous depositions and also to assure a practically constant deposition temperature of the substrates during film formation.

After film deposition, all samples were subjected to annealing experiments in vacuum. The annealing studies were carried out in a secondary vacuum furnace, after its evacuation to about 10^{-4} Pa. The selected temperature range varied from 300 to 800 °C, and the isothermal time was fixed to 60 min, after the required heating time at 5 °C/min. The samples were allowed to cool down in vacuum before their removal to ambient environment.

The chemical composition of the coatings was investigated with a Cameca SX-50 Electron Probe Micro Analysis (EPMA), operating at 15 keV. The elemental quantification was performed by comparing the peak intensity in the sample with standards for each element, and applying a ZAF correction to the results. The chemical uniformity of the films throughout their entire thickness (<300 nm) was check by Rutherford backscattering spectrometry (RBS) carried out in a IBA Data Furnace NDF v9.2e at 2 MeV with He⁺⁺ with an scattering angles of 140° (standard detector) and 180° (annular detector) and incidence angles of 0 and 20° [13]. The structure and the phase distribution of the coatings were analyzed by X-ray diffraction (XRD), using a Philips PW 1710 diffractometer (Cu-K$_\alpha$ radiation) operating in a Bragg–Brentano configuration. The XRD patterns were deconvoluted, assuming to be Voigt functions to yield the peak position,

integrated intensity and integrated width (IntW). These parameters allow calculating the interplanar distance, preferential orientation and grain size. The color and reflectivity characterization were computed using a commercial MINOLTA CM-2600d portable spectrophotometer (wavelength range from 400 to700 nm), using diffused illumination at a viewing angle of 8°. The spectrophotometer was equipped with a 52 mm diameter integrating sphere and 3 pulsed xenon lamps. Color specification was computed under the standard CIE illuminant D65 (especular component excluded) and represented in the CIE 1976 $L^*a^*b^*$ (CIELab) color space [14,15].

3. Results and discussion

3.1. As-deposited films

The fundamental characteristics of the three co-deposited Au:TiO₂ series are presented in Table 1. During this work, the films will be denoted as is ascribed in Table 1.

Considering the chemical composition, the EPMA analysis revealed that the Au content ranged from 10 to 30 at.%, showing a linear relationship between the number of Au pieces in the Ti target and the Au content in the films. All films from the three different series presented compact morphologies, which can be classified as very dense T type from Thornton zone model or featureless [16]. In respect to the as-deposited structure, Fig. 1, all films exhibit broad and low intensity X-ray diffraction peaks. It is noticed that the breadth and intensity of the of the Au peaks decrease with the decrease of Au content in the films. For films containing Au contents up to 20 at.%, the two broad peaks centered at 2θ of 38.2° and 44.4°, fits quite well to the (111) and (200) reflections of the fcc-Au phase [ICDD 04-0787], respectively. Beside the features of (100) silicon substrates, no diffraction peaks were obtained from any known crystalline phase of the binary Ti–O compounds. Thus, it can be concluded that the microstructure of the Au:TiO₂ films consist of elementary Au building blocks immersed into an amorphous titanium oxide matrix, in agreement to the results of other authors [17]. Furthermore, both EPMA and RBS confirmed that the titanium oxide phase is approximately stoichiometric.

Nevertheless it is important to notice that, in the as-deposited state, the variation of the Au volume fraction (achieved by using theoretical approximation [18]) as well as the correspondent clusters diameter, do not display important optical characteristics. In fact, the films from A and B series (with the highest Au amounts) revealed an intrinsic-like grey color, with no apparent differences between them. Regarding the films from series C (the one with the lowest Au content), the visual inspection of its surface revealed a blue-gray tone, characteristic of an interference-like behavior, consistent with the overall results that will be shown latter on this paper in the respective reflectivity curves. The relatively low Au content in this sample and the correspondent large stoichiometric TiO₂ matrix are consistent with this type of behavior.

3.2. Annealed coatings

After deposition, all the films were submitted to thermal annealing in protective (vacuum) atmosphere up to 800 °C. The main idea was to promote some structural and morphological changes in the films,

Table 1
General conditions and characteristics of deposited films.

Film series	Au pellets	Thickness (nm)	Au (at.%)	Au volume fraction, f_{Au}[a]
A	6	270	29.2	0.41
B	4	320	19.8	0.29
C	2	250	9.3	0.15

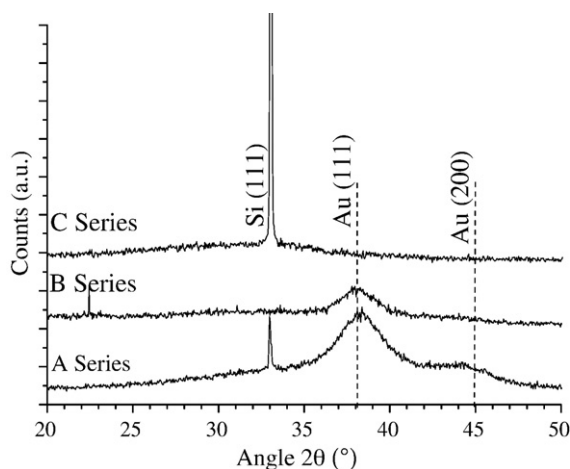[a] Considering $\rho(Au) = 19.3$ g/cm³ and $\rho(TiO_2) = 4$ g/cm³.

Fig. 1. XRD pattern of the as-deposited Au:TiO₂ films with (A) 29.2 at.% Au (B) 19.8 at.% Au and (C) 9.3 at.% Au.

namely the change of the Au clusters size and their distribution on the dielectric TiO₂ surrounding medium and, consequently, to analyze the change of the optical properties of the films. Fig. 2 shows the reflectivity measurements for films from series A, both as-deposited and after annealing at 300 °C. For comparison purposes, a sample of bulk gold was also analyzed. As expected, the films present clear evidences that the Au content, close to 30 at.%, could be already in the upper limit to observe any optical interesting features, namely concerning its sensitivity to the SPR effects. In fact, the occupancy of about 40% of the total film volume by the Au phase (Table 1), and the coalescence of them, leads to a golden-like appearance of the surface after thermal annealing at temperatures as low as 300 °C. Moreover, and consistent with the relatively high volume fraction, the optical behavior of the post-annealed series A is actually very similar to that obtained for "pure" gold (Fig. 2). The higher reflectivity of the "pure" gold sample is due to its bulk morphology. As reported for "pure" TiO₂ films, the reflectivity of the as-deposited film does not show any unexpected optical behavior. Furthermore, it is also important to clarify that the "pure" TiO₂ films are known to show no remarkable optical behavior changes, even when heat treated at high annealing temperatures [19].

Similar to the metal free-TiO₂ thin films [20], the reflectivity of the 29.2 at.% Au:TiO₂ films shows no important changes in the optical behavior after thermal treatments up to 800 °C. The similarity of the series A optical reflectivity upon annealing can be understood from the structural changes observed by XRD investigation. Analyzing the
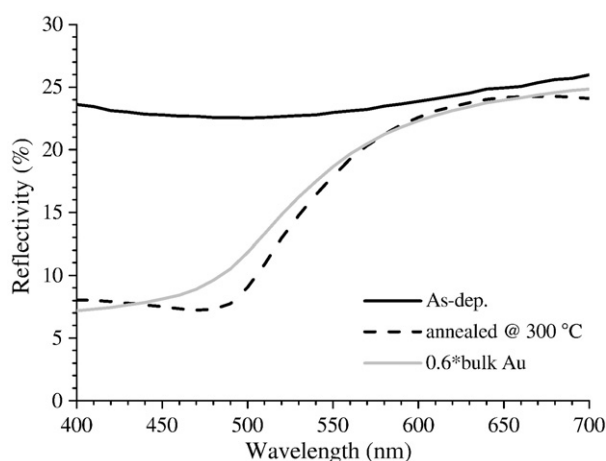
structural evolution as function of the annealing temperature, Fig. 3, it can be concluded that the well defined crystalline fcc-Au structure is immediately achieved for a temperature as low as 300 °C. The XRD peaks of the metallic gold, (111) and (200), become narrower and more intense, which is a behavior that is characteristic of some recrystallization and grain growth processes. However, no significant Au crystallite size variation is observed during heating from 300 to 800 °C. Thus, these high Au content annealed thin films do not loose their nano-characteristics, presenting a mean grain size which increases from roughly 3–4 nm in the as-deposited sample to about 23–25 nm, when samples were annealed from 300 to 800 °C. These results are in straight agreement with those obtained by optical reflectivity characterization, which actually show also a notorious constancy after annealing from 300 to 800 °C, in comparison to the as-deposited sample. The main feature in this series of thin films seems to be that related with the occurrence of coalescence of the Au particles, which due to the high grain sizes decrease the probability of SPR appearance.

Regarding the films from series B, with a Au content of 19.8 at.% (corresponding to a volume fraction of about 29% (Table 1)), the investigation revealed the most interesting results in terms of structural and morphological features, and consequently in terms of the optical properties variation. The first important set of results that are worthy to be mentioned are those related with the color coordinates and reflectivity. In fact, the surface coloration evolved from a dark grey tone, characteristic of the as-deposited films, to a red-brownish color tone after the annealing treatment at 300 °C. With the increase of the annealing temperature, the samples were firstly found to reveal some darkening of their surface red tones, and finally to turn golden-yellow for annealing temperatures above 600 °C. These visual colour changes were confirmed by the CIELab measurements, as illustrated in Fig. 4.

In fact, the analysis of this figure allows grouping the chromaticity coordinates into three distinct zones, matching these coloration changes with those observed by direct inspection of the samples surface. For the first thermal annealing, carried out at 300 °C, and similarly to what has been observed for the samples from series A, a clear change of all color coordinates is observed when compared to those obtained in the as-deposited sample (zone I). The region containing the samples annealed at these first temperatures, denoted as zone II, congregate all the samples annealed up to 600 °C; and it is characterized by a slight increase of both a^* (redness) and b^* (yellowness) coordinates and a two-fold behavior of the L^* parameter. For higher annealing temperatures, $T > 600$ °C, the b^* values are kept approximately constant, while a^* values show a slight decrease. This is in agreement with the color changes from the red-brownish tone to
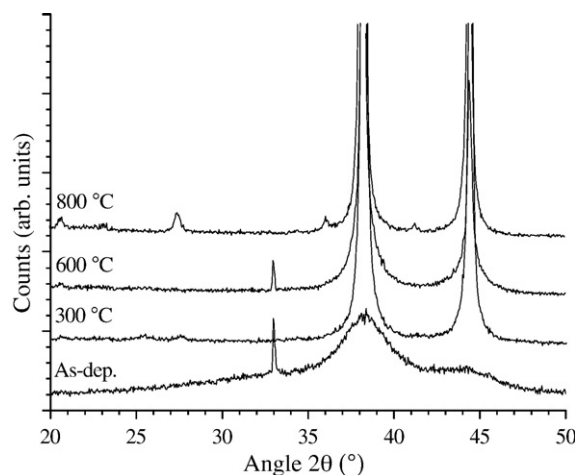

Fig. 2. Reflectivity on the visible spectrum of the 29.2 at.% Au:TiO₂ films from series A (as-deposited and post-annealed at 300 °C), compared with a Au bulk sample.

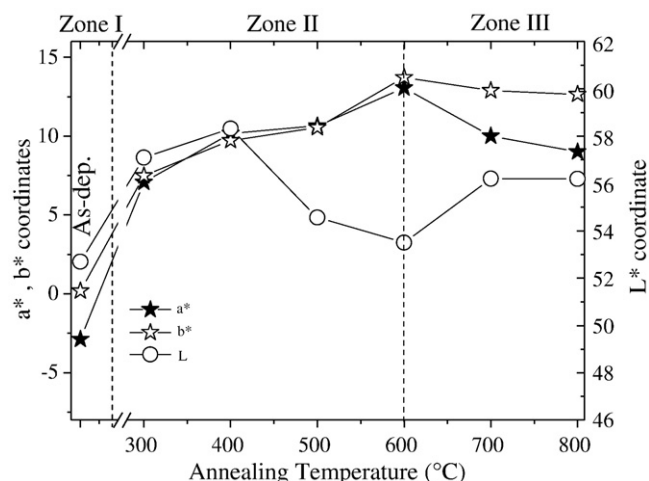**Fig. 3.** Structural evolution of the A series films as a function of the annealing temperature.

Fig. 4. CIELab 1976 color space chromaticity coordinates versus the annealing temperature for the samples from B series.

the golden-like surface. The samples that evolved to a golden-yellow region was designated as zone III, being also characterized by an increase of the L^* values coincident with the brighter golden-like tone that the samples presented.

The evolution of the CIELab parameters for annealed films are also in accordance with the reflectivity behavior presented in Fig. 5A), confirming the significantly different reflectivity behavior that was observed in the annealed samples when compared to the as-deposited one, as it was also observed in the samples from the previous series. As a general trend, it can be observed that the decrease of the reflectivity for the low wavelength range (up to <500 nm) is then followed by a significant increase for wavelength above 500 nm, where a minimum seems to occur in its vicinity for all samples. Anyway, and due to the relatively close behaviors, the derivative of the reflectivity spectra, which is presented in Fig. 5B), is a better option to show the different behaviors of the reflectivity curves. A first observation that can be drawn form the set of these two plots is that there are non-neglecting shifts that can be detected in the maximum peak position, in opposite to the minimum of reflectivity that are located, as mentioned, at almost the same wavelength value for all the thermally annealed films, Fig. 5A). The minimum in reflectivity corresponds to a derivative zero value in the Fig. 5B). Furthermore, it is also evident from the analysis of Fig. 5B) that the trend of the derivative spectra, located between 480 and 510 nm, shows a higher slope with the increase of the annealing temperature, so a higher reflectivity rate is reported, the reflectivity per wavelength unit is higher. Therefore, considering the groups defined previously for 19.2 at.% Au:TiO$_2$ films chromaticity coordinates, the following conclusions could be drawn:

Zone I — the as-deposited samples reveal an almost constant and relatively low reflectivity (between ∼20.2 and 24.0%) in the visible region, justifying the observed grey colour.

Zone II — the samples annealed at temperatures up to 600 °C reveal that the locations of the reflectivity minima are slightly shifting to higher wavelengths, when the annealing temperature increases from 300 to 600 °C (480.0 nm at 300 °C to 490.1 nm for 600 °C). This fact is in accordance with the red-brownish tone detected by the CIELab coordinates for the samples. The darkness of the red-brownish coloration with the increase of the annealing temperature is in agreement with the decrease of the reflectivity at higher wavelengths. Another important observation is the difference between the reflectivity values in the wavelength range between 480 and 510 nm. In general, the higher the annealing temperature is, the higher the slope values are and, thus, the

higher is the reflectivity. As a consequence, either it could give rise to a change in the tone that can disguised the lower reflectivity in that region, for the samples annealed at 500 and 600 °C, or the shifting of the maximum for lower wavelengths (570 nm for 300 °C and 530 nm for 600 °C).

Zone III — for the samples that were thermally annealed at temperatures above 600 °C, a further increase of the reflectivity values between 480 and 510 nm is detected, with the maximum occurring at slightly lower wavelengths (in the border of the green region of the visible spectrum). Thus, in this region, the reflectivity is very high, approaching the optical behavior for "pure" gold, and in consequence, the appearance of the gold-like tones on the films annealed at 700 and 800 °C.

In order to validate the contribution of the structural/morphological changes in the observed optical behavior, an extensive set of XRD experiments were carried out. Fig. 6 shows the diffraction patterns obtained after thermal annealing for temperature up to 800 °C in vacuum. The analysis of this figure allows concluding that important phase transitions in addition to structural parameters variations are presented after annealing process. The first important note that is worth being mentioned is that by allowing diffusion and coalescence phenomena, the thermal annealing leads to a progressive growing of the Au clusters. In fact, the enhancement of the intensity and the narrowing of the XRD peaks assigned to the fcc-Au phase as the annealing temperature increases are evident, in opposition to the as-deposited state, characterized by a very broad and low intensity (111) reflection of metallic gold. Moreover, and as can be observed in Fig. 6, besides the well defined diffraction peaks of the fcc-Au, the others, of minor intensity, can be indexed as TiO$_2$ phase (see Fig. 6). This result clearly indicates that the thermal treatments at temperatures above 400 °C also give rise to the crystallization of the dielectric TiO$_2$ matrix. Pure anatase phase [ICDD 21-1272] is detectable at 400 °C and persists up to 600 °C. XRD peaks are very broad indicating small size nanocrystalline TiO$_2$ particles [21]. At 600 °C, rutile related peaks [ICDD 21-1276] started to appear and a mixture of both anatase and rutile phases are present in the samples from this B series. No anatase related peaks are observed at or above 700 °C, indicating a complete phase transformation from anatase to rutile. The correlation is clear, though the shape of Au (200) peaks, especially at 500 °C, could indicate the presence of a bimodal distribution of the grain size. On the TiO$_2$(Au) films, with nanoparticles under approximately 4 nm, the collective oscillation is confined to a ultrafine grains obtained during the deposition [22]. These results are in agreement with those reported for crystallization of Ti–O sputtered films [17] and for Ag:TiO$_2$ studies [20] that showed changes from the theoretical phase transformation temperatures [20,21].

Important also to note is that both phases coexist at 600 °C, exactly where the optical behavior changes are more severe. Au clusters accelerate the anatase–rutile transformation at this Au concentration, as happens with Ag nanoclusters at lower concentrations [23]. This result confirms that not only the type of clusters, their distribution and shape, but also the nature of the dielectric matrix are affecting the optical behaviour of these type of systems having a non-neglecting effect on the energy as well as on the width of the surface plasmon resonance [23,24], tuning the optical properties of the film. Moreover, both anatase and rutile phases reveal some differences in their optical characteristics. Rutile has a refractive index that varies from 2.42 to 2.66, while the anatase phase is characterized by a range of 2.33–2.38 [20]. Change in the matrix structural arrangement may also play an important role for the observed optical behavior of the B series films. A clear correlation between cluster grain size and their SPR is discussed on the final step of this section.

Regarding the set of samples from series C, having an Au fraction volume of about 15% (corresponding to an Au content of 9.3 at.%), Fig. 7 presents the CIELab chromaticity evolution as a function of annealing temperature. The first noticeable result is that the as-deposited sample
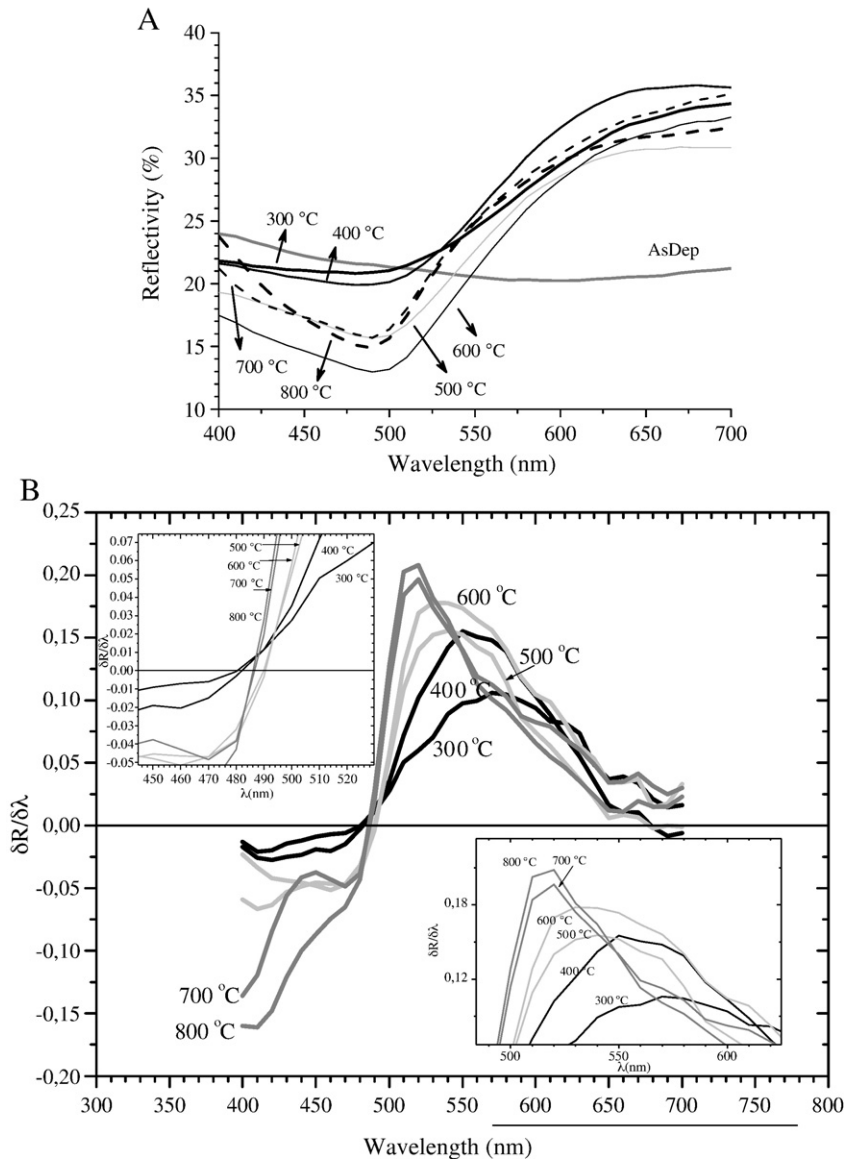
Fig. 5. A). Reflectivity on the visible spectrum of samples B at different annealing temperatures. B). Derivative and details of the reflectivity spectra (A).
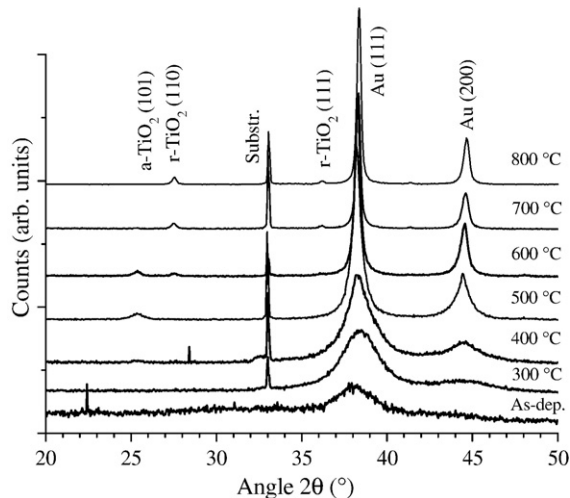

Fig. 6. XRD diffractograms of samples from series B at different annealing temperatures.

showed a blue interference-like tone, which changed with the annealing experiments to a red-brownish tone. However, and as revealed in all cases, there were some traces of the interference optical behavior, which remained on the annealed samples reflectivity curves. Due to this apparent interference-like behavior, this figure should be analyzed carefully, since the measured values may be affected by this particular type of behavior. In this series, the intrinsic golden-like color was never reached, even for the highest annealing temperatures, in opposition to that observed for series A and B. As a first conclusion, one might claim that this concentration regime (below 10 at.% of Au) is already in the lower limit of concentration to have an intrinsic response of this kind of nanocomposites.

For annealing temperatures higher than 500 °C, a^* reaches the highest values, which can explain the red-brownish color observed in the samples. Anyway, and as mentioned, the apparent interference-like behavior of the samples from this series does not allow an accurate separation of the samples in terms of their particular color. The interference behavior of color was also confirmed on the reflectivity curves presented in Fig. 8. Though the interference-like behavior seems to persist for all annealing temperatures, the as-deposit sample has a total interference optical behavior which seems to be smoothened at higher annealing temperatures.
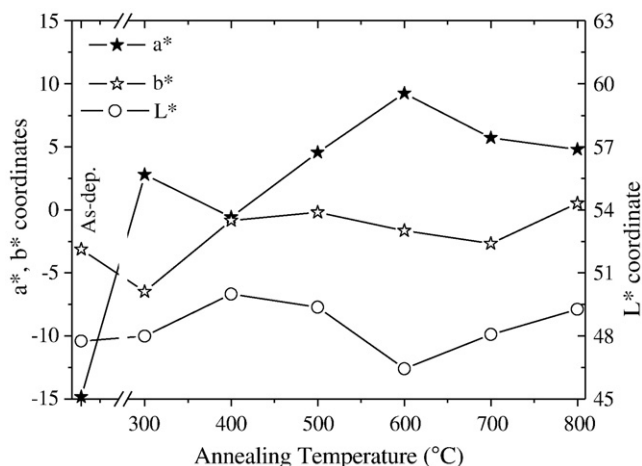
Fig. 7. CIELab values versus the annealing temperature for the C conditions samples.

Fig. 9. XRD difractograms of sample C at different annealing temperatures.

In order to follow the structural changes that may have occurred, a detailed XRD analysis was carried out. The first important result, and confirming the quite different behavior obtained for these samples in comparison to those of series A and B, is that also the diffraction patterns seem to follow a different trend, particularly in the case of the dielectric-base matrix. XRD analyses show the anatase–rutile transformation with the annealing temperature (Fig. 9). This transformation occurs at different temperatures in B and C series. The different size and amount of Au clusters affect the TiO_2 phase transformations. At temperatures higher than 600 °C Anatase peak are not presents on B series, although it is already present at 800 °C for C series. Higher amounts of gold particles (series B) promote the phase transformations at lower temperatures [25], while the different phases composition on the matrix also affect the SPR [26].

The low Au content in addition to the low nanoparticles dimension developed during thermal treatments, places C series in a border behavior between a typical interference thin film behaviour (as is the case of metal-free TiO_2 films) and the optical SPR nanocomposite conditions (reached in this work for addition of 19.2 at.% Au). In fact, the variation of the Au clusters size on the C samples never reaches the limit of ~15 nm, value for which the main optical changes appeared in films of the B series, as can be confirmed in Fig. 10.

The trend in the variation of the cluster dimension is similar in all the sputtered Au:TiO_2 films, where the main feature is that related with an increase that is observed with increasing annealing temperatures
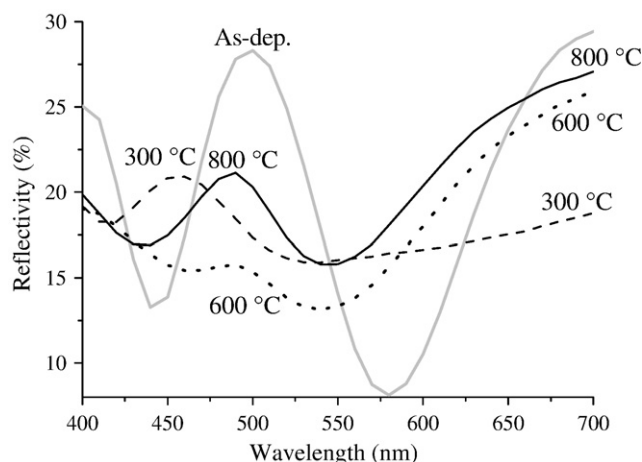
(Fig. 10). Nevertheless, there seem to be some clear differences between then three series. The results from the samples indexed to series B show a critical nanoparticle size when the SPR and the optical changes are evident due to a high clusters interaction. SPR effects might be present on the first annealed samples but are more evident at 600 °C annealed samples corresponding to 15–20 nm of clusters size [27]. Clusters uniformity is shown as a key factor to reach SPR phenomenon, which changes the optical behavior of the film. At low annealing temperatures the SPR is low, due to interaction among the nanoparticles. Higher annealing temperatures lead to higher grain size and increase the distances between the Au clusters. At 600 °C they reach the optimal distance and the SPR effects are more intense.

Coalescence between Au nanoparticles could give the golden appearance color observed in films with Au content higher than 20 at.%. For the particular case of B series, it seems that this "critical" grain size, where the SPR seems to happen for 15–20 nm, is obtained after the heat treatment at 600 °C. The coalescence will decrease the probability of particles interaction giving the golden appearance. On the studied system SPR only takes place with cluster lower sizes than 22–24 nm. For higher temperatures, and consequently for higher clusters sizes, the 19.2 at.% Au:TiO_2 films become golden-like, similarly to A series (300 °C), meaning that the thermal conditions might be above those required to observe SPR.

As shown in Fig. 10, Au clusters are confined on the nanometrical scale, and their average size is growing with the increase of the

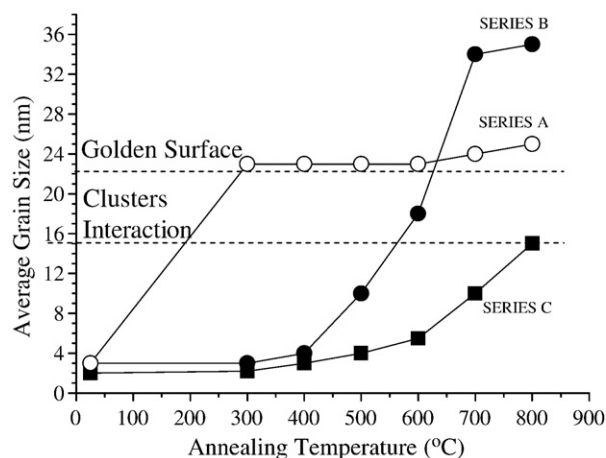**Fig. 8.** Reflectivity on the visible spectrum of samples C at different annealing temperatures.

Fig. 10. Comparison of the size grain growh of three films series and their correlation with the SPR optical effects.

annealing temperature. The SPR frequency and the consequent optical properties are very sensitive to the shape and size distribution of the Au clusters [28]. This figure clearly illustrates the grain size growing during the annealing treatments, especially after 300 °C, where the main reflectivity changes are reported (Fig. 5). The reflectivity at nominal wavelength becomes stronger with the growth of the small Au particles, as it happens with the absorbance at lower wavelength. Anyway, it is important to emphasize that in spite of the only slight increase of grain size that Fig. 10 indicates for the annealing up to 500 °C, it is to admit that this apparent slight growth might be hidden by the shape of the diffraction peaks itself, i.e., the grain size values could be modified due to some bimodal size distribution. The growing process could be non-homogeneous and some particles grow while others keep the as-deposited size. It is already known that a narrow distribution has a more sensitive response. Some coalescence between Au as-deposited particles is also present. The particle growth heterogeneous process is a possible explanation for the unsymmetrical shape of the XRD peaks of the 400 °C and 500 °C difractograms, shown on Fig. 6. At 500 °C, the peak becomes narrower because there is a predominant grain size, larger and more crystalline, which is more sensitive to the particles interaction, giving the main SPR. This fact is linked with the main changes on the reflectivity and color analysis. The 300 °C annealed sample shows that the grain size is quite similar to those obtained in the as-deposited sample, which means that the significant changes that were observed in optical characteristics (reflectivity and CIELab color coordinates, Figs. 4 and 5) are mostly due to the redistribution or agglomeration of Au nanoparticles, and some grain growing that may occur, even the hypothetical bimodal morphology hide the possible field resonance. The golden like surface appears at grain sizes higher than 22–24 nm, which has a higher size than the reported on the samples from series A, for annealing at 300 °C. This result induces that, in fact, a mixture of composition and grain morphology are ruling the changes on the percolation responsible of the SPR, and due to this tunable SPR, the changes on the optical responses were obtained [29]. The rapid growth of the clusters can be due to the high diffusion. It is clear that at Au concentrations between 30 at.% and 10 at.%, the SPR and color of the Au:TiO$_2$ thin films can be tuned by annealing treatments since they monitor the grain size and distribution of the Au clusters on the dielectric matrix.

4. Conclusions

The "One Step" Co-Sputtering technique of Ti–Au target were highlighted as one of the most useful way to obtain sensitive films structures to optical change, with the proper volume particles fraction and particle size to reach SPR interactions.

Reflectivity percentages on the visible spectrum range and CIELab color values show a direct relation with the annealing temperature which is changing the grain size of gold clusters embedded in the dielectric matrix.

The interaction of the gold nanoparticles, and in consequence the color of the nanocermet thin films, can be monitored by the grain size of the Au nanoparticles which shows a rapid growth with the annealing heat treatments in vacuum.

Concentrations of 20 at.% are showed as the most sensitive films with the most interesting results. The changes of their optical behavior

and color are evident at the first annealing temperatures and show a wide range of optical behavior until the golden like surface is reached.

Clusters size between 12 and 22 nm produce optical changes due to their interaction on the dielectric matrix. At higher sizes golden appearance is reported on the surface. The main optical changes are observed at annealing temperatures around 500–600 °C with average grain size around 10 nm.

Acknowledgments

References

[1] Peng Zhou, Hai Yang You, Jian Hu Jia, Jing Li, Tao Han, Song You Wang, Rong Jun Zhang, Yu Xiang Zheng, Liang Yao Chen, Thin Solid Films 455–456 (2004) 605.
[2] M. Gajdardziska-Josifovska, R.C. McPhedran, D.J.H. Cockayne, D.R. McKenzie, R.E. Collins, Appl. Opt. 28 (1989) 2736.
[3] Thearith Ung, Luis M. Liz-Marzan, Paul Mulvaney, J. Phys. Chem., B 105 (17) (2001) 3441.
[4] Eduardo Coronado, Lin Lin Zhao, George C. Schatz, K. Lance Kelly, J. Chem. Phys. 107 (2009) 668.
[5] E. Hutter, Janos H. Fendler, Adv. Mater. 16 (2004) 1685.
[6] V. Shutthanandan, Y. Zhang, S. Thevuthasan, L.E. Thomas, W.J. Weber, G. Duscher, C.M. Wang, Nucl. Instrum. Methods Phys. Res. Sect. B 242 (2006) 448.
[7] Lidia Armelao, Davide Barreca, Gregorio Bottaro, Alberto Gasparotto, Silvia Gross, Cinzia Maragno, Eugenio Tondello, Coord. Chem. Rev. 250 (11–12) (2006) 1294.
[8] Dan Dalacu, Ludvik Martinua, J. Appl. Phys. 87 (2000) 442.
[9] Minyung Lee, Lee Chae, Kyeong Chul Lee, Nanostruc. Mater. 11 (2) (1999) 195.
[10] U. Kreibig, M. Vollmer, Optical Properties of Metal Clusters, Springer-Verlag, Berlin, 1996.
[11] A. Dakka, J. Lafait, M. Abd-Lefdil, C. Sella, M. Maaza, Eur. J. Appl. Physiol. 9 (2000) 105.
[12] N. Martin, C. Rousselot, D. Rondot, F. Palmino, R. Mercier, Thin Solid Films 300 (1997) 113.
[13] N.P. Barradas, C. Jeynes, R.P. Webb, Appl. Phys. Lett. 71 (1997) 291.
[14] Colorimetry, CIE Publ. 1971 (Commission Internationale de L'Éclairage) 15.
[15] Recommendations on Uniform Color Spaces, Difference–difference equations, psychometric color terms, CIE Publication (Commission Internationale de L'Éclairage) 1978 2–70 15.
[16] J.A. Thornton, Annu. Rer. Mater. Sci. 7 (1977) 239.
[17] M.G. Manera, J. Spadavecchia, D. Buso, C. de Julbn Fernbndez, G. Mattei, A. Martucci, P. Mulvaney, J. Pqrez-Juste, R. Rella, L. Vasanelli, P. Mazzoldi, Sens. Actuators, B, Chem. 132 (1) (2008) 107.
[18] Juan Wang, W.M. Lau, Quan Li, J. App. Phys. 97 (11) (2005) 114303.
[19] Hiroshi Yoshida, Hiroyuki Nasu, Kanichi Kamiya, Jun Matsuoka, J. Sol-Gel Sci. Technol. 9 (2) (1997) 145.
[20] Hemissi, H. Mardjia-Adnani, J.C. Plenet, Curr. Appl. Phys. 9 (4) (2009) 717.
[21] A.N. Sprafke, H. Dieker, M. Wuttig, G. von Plessen, C. Dahmen, J. Appl. Phys. 88 (2006) 011923-1-3.
[22] M. Hemissi, H. Mardjia-Adnani, J.C. Plenet, Curr. Appl. Phys. 9 (4) (2009) 717.
[23] J. Garcia-Serrano, E. Gómez-Hernbndez, M. Ocampo-Fernández, U. Pal, Curr. Appl. Phys. 9 (5) (2009) 1097.
[24] S.K. Mandal, R.K. Roy, A.K. Pal, J. Phys. D, App. Phys 36 (3) (2003) 261.
[25] Thiel, S. Ismat, ShahA. Ahmad, J. Phys. Conf. Ser. 61 (2006) 11.
[26] Seung Wan Ryu, Eui Jung Kim, Seung Kook Ko, Sung Hong Hahn, Mater. Lett. 58 (5) (2004) 582.
[27] S.K. Mandal, R.K. Roy, A.K. Pal, J. Phys. D, App. Phys. 35 (17) (2002) 2198.
[28] S. Lee, D.Y. Kub, T.S. Leec, B. Cheongc, W.M. Kimc, K.S. Leec, S.H. Cho, Thin Solid Films 447–448 (2004) 68.
[29] Sunghun Cho, Soonil Lee, Soo ghee Oh, Sung Jin Park, Won Mok Kim, Byungki Cheong, Moonkyo Chung, Ki Bong Song, Taek Sung Lee, Soon Gwang Kim, Thin Solid Films 377–378 (2004) 97.